8th Biennial International Conference
& Exposition on Petroleum Geophysics

"HYDERABAD 2010"

P-402

AVO and pre-stack inversion

Brian Russell, Hampson-Russell, *CGGVeritas Company, Calgary, Alberta*

Summary

The Amplitude Variations with Offset (AVO) technique has grown to include a multitude of sub-techniques, each with its own assumptions. AVO techniques can be subdivided as either: (1) seismic reflectivity or (2) impedance methods. Seismic reflectivity methods include: near and far stacks, intercept versus gradient analysis and the fluid factor. Impedance methods include: P and Simpedance inversion, Lambda-mu-rho (LMR), and Elastic Impedance. The objective of this talk is to make sense of all of these methods and show how they are related.

Introduction

Figure 1 shows the relationship between geology and geophysics for a simple layered earth. The geologist typically looks at some parameter measured by a well log tool, whereas the geophysicist looks at the reflectivity derived from this parameter.

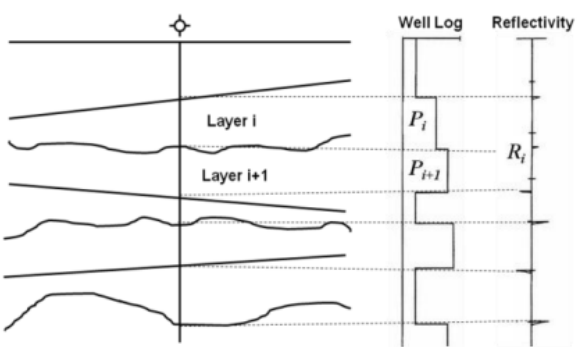

Figure 1. The relationship between geology and geophysics, where geologists look at some parameter P and geophysicists measure the reflectivity R.

The relationship between the parameter and the derived reflectivity can be written:

$$R_i = \frac{P_{i+1} - P_i}{P_{i+1} + P_i} \approx \frac{\Delta P_i}{2\overline{P}_i}, \quad (1)$$

where: $\Delta P_i = P_{i+1} - P_i$ and $\overline{P}_i = \frac{P_{i+1} + P_i}{2}$.

But which parameter P are we interested in? To the geophysicist the choices usually are: P-wave velocity (V_P), S-wave velocity (V_S), Density (ρ,) and transforms of velocity and density such as acoustic impedance (V_P) and shear impedance (V_S). The geologist would add parameters like gamma ray, water saturation, and so on. Typically, AVO reflectivity techniques allow us to extract and analyze different types of reflectivity, whereas impedance techniques allow us to transform back to the parameter itself.

Reflectivity methods

Seismic reflectivity methods are based on the Aki-Richards equation (Aki and Richards, 2002):

brian.russell@cggveritas.com

$$R_P(\theta) = aR_{VP} + bR_{VS} + cR_D, \qquad (2)$$

$$\text{where}: R_{VP} = \frac{\Delta V_P}{2\overline{V}_P},\ R_{VS} = \frac{\Delta V_S}{2\overline{V}_S},\ R_D = \frac{\Delta\rho}{2\overline{\rho}},$$
$$a = 1 + \tan^2\theta,\ b = -8K\sin^2\theta,\ c = 1 - 4K\sin^2\theta,$$
$$\text{and } K = \left(\frac{\overline{V}_S}{\overline{V}_P}\right)^2.$$

Fatti et al. (1994) re-formulated this equation as

$$R_P(\theta) = aR_{AI} + bR_{SI} + c'R_D, \qquad (3)$$

$$\text{where } R_{AI} = \frac{\Delta AI}{2AI} = R_{VP} + R_D,\ AI = \rho V_P,$$
$$R_{SI} = \frac{\Delta SI}{2SI} = R_{VS} + R_D,\ SI = \rho V_S, \text{ and } c' = 4K\sin^2\theta - \tan^2\theta.$$

They also defined fluid factor ($\triangle F$) as:

$$\Delta F = R_{AI} - gR_{SI}, \quad \text{where } g = 1.16(V_S / V_P) \qquad (4)$$

Another popular re-expression of the Aki-Richards equation, derived by Shuey (1985), is given by:

$$R_P(\theta) = R_{AI} + G\sin^2\theta + R_{VP}\sin^2\theta\tan^2\theta, \qquad (5)$$

where : $G = R_{VP} - 8KR_{VS} - 4K_{RD}$ = the gradient
and R_{AI} is the intercept

To implement the mathematical schemes given in equations 2 through 5, we first pick the seismic values in the prestack domain, as shown in Figure 2, and fit the three reflectivity parameters using least-squares methods. The results can then be displayed for further analysis.

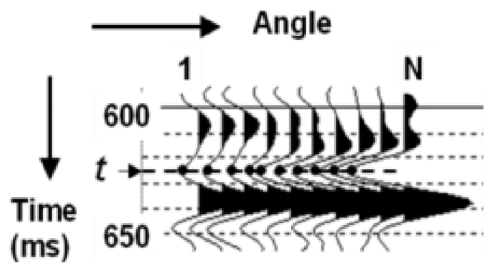

Figure 2. Seismic amplitudes are picked from pre-stack gathers and then fit to the models given in equations 2 through 5 using a least-squares approach.

For example, Figure 3 shows a crossplot of the intercept versus gradient values from equation 5, and Figure 4 shows a plot of the highlighted regions back on the seismic crosssection. The pink zone shows the top-of-gas, the yellow zone shows base-of- gas, and the blue zone shows a "hard – streak" which is not hydrocarbon bearing .

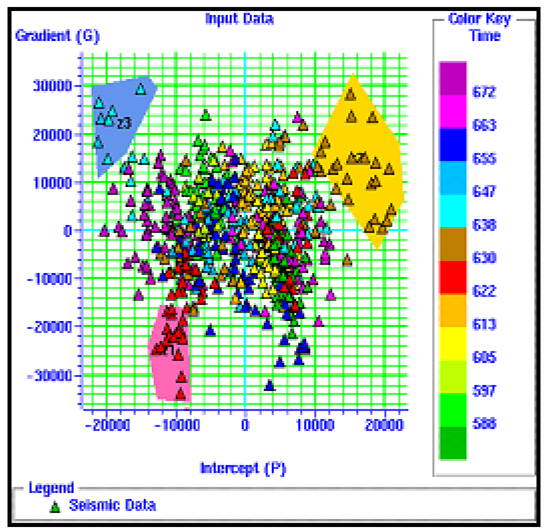

Figure 3. A cross-plot of intercept versus gradient for a gas-sand example from Alberta. The coloured zones represent potential anomalies.

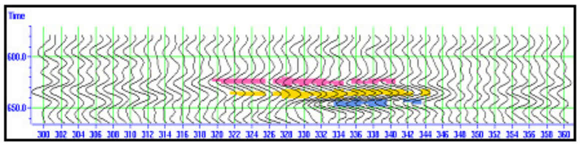

Figure 4. The zones from Figure 3 superimposed on the original seismic section, where pink shows top-ofgas, yellow shows base-of-gas and blue shows a nonhydrocarbon bearing hard streak.

Impdedance Methods

The reflectivity methods just described can be thought of as "classical" AVO More recently, inversion techniques have be applied to the reflectivity functions shown in equations 2, 3 and 5 to produce broad-band impedance estimates.

These methods are an extension of classical post-stack impedance methods (Russell and Hampson, 1991) in which only acoustic impedance was extracted. More recently, using an extension of equation 3, we can simultaneously extract broad-band estimates of acoustic impedance, shear impedance and density (Hampson et al, 2005). From these impedances, other parameters of interest like *Vp/Vs* ratio, $\lambda\rho$ and $\mu\rho$ (Goodway et al., 1997) and more generalized fluid property attributes (Hampson et al., 2003) can be extracted. For example, Figure 5 shows the low *Vp/Vs* ratio associated with a gas sand, found using the simultaneous pre-stack inversion technique.

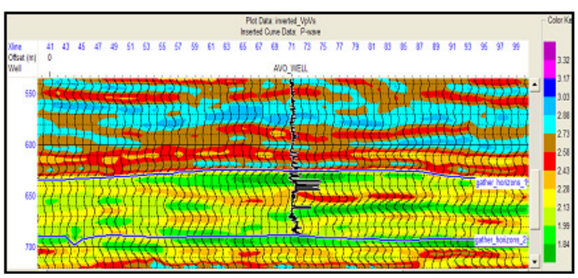

Figure 5. A broad-band estimate of Vp/Vs ratio using the simultaneous pre-stack inversion technique, where the low impedance in the centre of the section below the first picked event is representative of a gas sand.

Another approach to inversion is the concept of Elastic Impedance, or *EI*, (Connolly, 1999) which gives us a quantitative way of analyzing near and far angle stacks. This method uses equation 1 to show that:

$$R_{EI}(\theta) \approx \frac{1}{2}\frac{\Delta EI(\theta)}{EI(\theta)} \approx \frac{1}{2}\Delta \ln EI(\theta),\ EI(\theta) = V_P^a V_S^b \rho^c \qquad (6)$$

Figures 6 and 7 illustrate the *EI* method for the gas sand example we have been considering.

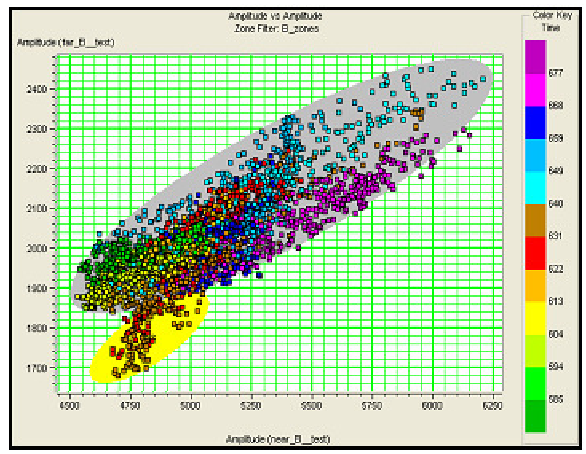

Figure 6. A cross-plot of near versus far elastic impedance.

The crossplot in Figure 6 shows *EI* at 7.5° on the horizontal axis, and *EI* at 22.5° on the vertical axis. The background trend is the grey ellipse, and the anomaly is the yellow ellipse. These zones are shown on the seismic section in Figure 7.

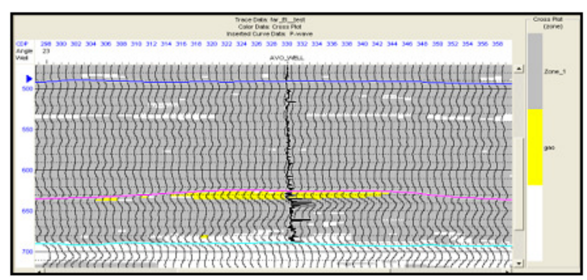

Figure 7. The zones from Figure 6 superimposed on the seismic section, where the yellow zone indicated gas and the grey zone is the wet background.

Whitcombe et al. (2002) extended the EI method and called it Extended Elastic Impedance, or EEI. EEI gives us the ability to extract other physical parameters such as the gamma ray response.

Conclusions

This talk has been an overview of the various methods used in the Amplitude Variations with Offset (AVO) technique. I showed that all of these methods are based on the AkiRichards approximation to the Zoeppritz equations. I then subdivided AVO techniques as either: (1) seismic reflectivity or (2) impedance methods. Seismic reflectivity methods are straightforward to derive and to interpret but do not give us physical parameters. Impedance methods are more difficult to derive but give us physical parameters including reservoir properties. A summary of the methods described in this paper is given in Figure 8.

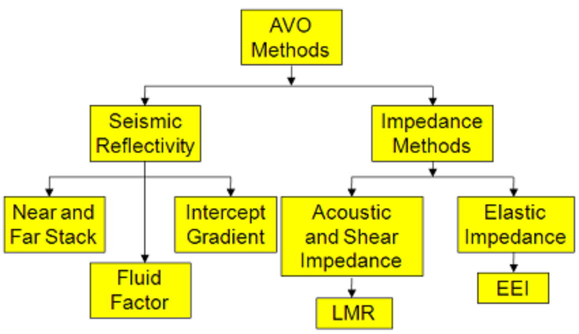

Figure 8. A summary of the methods described in this paper.

In the final analysis, there is no single "best" method for solving every exploration objective . Explorationists are urged to pick the method that works best in their area .

References

Aki, K., and Richards, P.G., 2002, Quantitative Seismology, 2nd Edition: W.H. Freeman and Company.

Connolly, P., 1999, Elastic impedance: The Leading Edge, 18, no. 4, 438-452.

Fatti, J., Smith, G., Vail, P., Strauss, P., and Levitt, P., 1994, Detection of gas in sandstone reservoirs using AVO analysis: a 3D Seismic Case History Using the Geostack Technique, Geophysics, 59, 1362-1376.

Goodway, W., Chen, T., and Downton, J., 1997, Improved AVO fluid Detection and Lithology Discrimination Using Lamé Petrophysical Parameters: Extended Abstracts, SEG 67th Annual International Meeting, Denver.

Hampson, D.P, Russell B.H., and Bankhead, B., 2005, Simultaneous inversion of pre- stack seismic data SEG, Expanded Abstracts, 24 , no. 1, 1633-1637.

Russell, B. and Hampson, D., 1991, A comparison of poststack seismic inversion methods: Annual Meeting Abstracts, Society Of Exploration Geophysicists, 876-878.

Russell, B., Hedlin, K., Hilterman, F. and Lines, L. R., 2003, Fluid-property discrimination with AVO: A BiotGassmann perspective: Geophysics, 68**,** 29-39.

Shuey, R.T., 1985, A simplification of the Zoeppritz equations: Geophysics 50, 609-614.

Whitcombe, D.N., Connolly, P.A., Reagan R.L. and Redshaw, T.C., 2002, Extended elastic impedance for fluid and lithology prediction: Geophysics, 67, no. 1, 63-67.